ISSN 1063-7729, Astronomy Reports, 2006, Vol. 50, No. 9, pp. 733–747. © Pleiades Publishing, Inc., 2006.
Original Russian Text © V.V. Bobylev, G.A. Goncharov, A.T. Bajkova, 2006, published in Astronomicheskiĭ Zhurnal, 2006, Vol. 83, No. 9, pp. 821–836.

The OSACA Database and a Kinematic Analysis of Stars in the Solar Neighborhood

V. V. Bobylev, G. A. Goncharov, and A. T. Bajkova

Central (Pulkovo) Astronomical Observatory, Russian Academy of Sciences, Pulkovskoe sh. 65, St. Petersburg, 196140 Russia

Received November 22, 2005; in final form, April 14, 2006

Abstract—We transformed radial velocities compiled from more than 1400 published sources, including the Geneva–Copenhagen survey of the solar neighborhood (CORAVEL–CfA), into a uniform system based on the radial velocities of 854 standard stars in our list. This enabled us to calculate the average weighted radial velocities for more than 25 000 HIPPARCOS stars located in the local Galactic spiral arm (Orion arm) with a median error of ±1 km/s. We use these radial velocities together with the stars' coordinates, parallaxes, and proper motions to determine their Galactic coordinates and space velocities. These quantities, along with other parameters of the stars, are available from the continuously updated Orion Spiral Arm Catalogue (OSACA) and the associated database. We perform a kinematic analysis of the stars by applying an Ogorodnikov–Milne model to the OSACA data. The kinematics of the nearest single and multiple main-sequence stars differ substantially. We used distant ($\bar{r} \approx 0.2$ kpc) stars of mixed spectral composition to estimate the angular velocity of the Galactic rotation, $\omega_\odot = -25.7 \pm 1.2$ km s^{-1} kpc^{-1}, and the vertex deviation, $l = 13^\circ \pm 2^\circ$, and detected a negative K effect. This negative K effect is most conspicuous in the motion of A0–A5 giants and is equal to $K = -13.1 \pm 2.0$ km s^{-1} kpc^{-1}.

PACS numbers : 98.35.Df, 98.35.Pr, 97.10.Wn
DOI: 10.1134/S1063772906090071

1. INTRODUCTION

Radial velocities of several tens of thousands of stars have been measured in recent years with precisions of better than ±1 km s^{-1}, making joint analyses of stellar proper motions and radial velocities of considerable importance for studies of stellar kinematics. An appreciable fraction of these high-precision radial velocities were measured using the CORAVEL photoelectric cross-correlation spectrometers and digital spectrometers of the Harvard-Smithsonian Cenrter for Astrophysics (CfA) and can be found in the catalog of Nordström et al. [1] (hereafter, the CORAVEL–CfA catalog). These authors and Gontcharov [2] showed that the combined use of proper motions and radial velocities, interstellar-extinction estimates, multicolor photometry, and binary parameters makes it possible to draw conclusions about the absolute magnitudes, ages, masses, and Galactic orbits of the stars and the evolution of Galactic structures over millions of years and to perform other stellar-kinematic studies. In order to systematically collect, analyze, and reduce the corresponding observational material, we have created and have been continuously updating our database for stars with known coordinates, parallaxes, proper motions, and radial velocities.

Although the mutual alignment and density of spiral arms in the solar neighborhood require a special study, intrinsically bright HIPPARCOS stars, which are tracers of the Galactic spiral arms, enable us to estimate fairly confidently the position and size of the local spiral arm. The HIPPARCOS catalog is complete to about 7.3^m in the band of the Milky Way, i.e., for stars with absolute magnitudes $M < -2^m$ located out to 600 pc, given that, as a rule, the extinction is lower than 0.5^m in this region. Moreover, stars with absolute magnitudes $M < -4^m$ belonging to neighboring spiral arms are represented almost completely in this catalog. The distribution of intrinsically bright stars over the Galactic octants and in the heliocentric distance presented in Table 1 indicates that, first, nearby intrinsically bright stars are distributed almost uniformly over the Galactic octants; second, such stars are not distributed uniformly in Galactic longitude at greater distances; and, third, the distribution changes abruptly at a heliocentric distance of more than 700 pc. Thus, within 400 pc from the Sun, only the Scorpio–Sagittarius association can be identified near a Galactic longitude of about 340°. At distances between 400 to 700 pc, intrinsically bright stars are mostly concentrated near latitudes of 90° and 225°, possibly indicating the directions to which

Table 1. Distribution of intrinsically bright stars (in percent) in the Galactic octants and heliocentric distance

Octant	$r < 400$ pc $M_V < -2$	$r < 500$ pc $M_V < -2$	400 pc $< r <$ 700 pc $M_V < -2$	$r > 800$ pc $M_V < -4$
0°–45°	11.1	9.9	9.3	10.5
45–90	11.0	12.8	17.7	14.1
90–135	12.5	14.2	17.4	19.7
135–180	11.4	10.9	10.8	11.2
180–225	13.1	13.7	13.0	12.3
225–270	11.4	13.6	14.8	8.9
270–315	12.5	11.5	9.5	15.1
315–360	17.0	13.3	7.5	8.2
Total number of stars	534	815	817	813

the local spiral arm extends, as well as the width of the arm, which is about ±500 pc in the directions of the Galactic center and anticenter. The predominant longitudes change beyond 800 pc: the regions of enhanced density of intrinsically bright stars near 110° and 290° correspond to the well-known Perseus and Sagittarius arms, respectively. We can thus refer to the region within 500 pc of the Sun as the portion of the local Orion arm that surrounds us.

Currently, radial velocities are known and parallaxes are relatively accurate primarily for stars within 500 pc of the Sun, i.e., within the local Galactic spiral arm (Orion arm). For this reason, we called the catalog based on our database the Orion Spiral Arm Catalog—OSACA (http://www.geocities.com/orionspiral/). The database, with its numerous tables, relations, and queries is a sort of "factory," whereas the final product that can be distributed is the OSACA catalog, which consists of several tables that are periodically compiled from the database.

The goal of this paper is to describe the catalog and to analyze the most interesting examples of its use for studies of the kinematics of stars in the solar neighborhood. One such example is analyzing the effect of an adopted model for the binarity of the nearest stars on their kinematic parameters. As another example, we considered relatively distant A0–A5 stars exhibiting a negative K effect. We performed our kinematic analysis using the Ogorodnikov–Milne model. We determined the Schwarzschild ellipsoid to analyze the residual velocities of the stars and construct two-dimensional distributions in the U, V plane.

2. CONTENT AND FORMAT OF THE OSACA CATALOG

The core of the OSACA catalog are the six quantities that describe the position and velocity of a star in space: α, δ, π, μ_α, μ_δ, and V_r. These quantities are used to calculate the coordinates X, Y, Z and the space velocities U, V, W [3] in the standard Galactic Cartesian coordinate system, where X increases toward the Galactic center, Y in the direction of Galactic rotation, and Z in the direction of the North Galactic Pole. The OSACA catalog is continuously updated with new published data. Every substantial change in the input data is followed by a recalculation of the dependent quantities; for example, the velocity components U, V, and W are recomputed after a refinement of the radial velocities in the database.

Since positions and velocities are known sufficiently precisely only for stars of the HIPPARCOS catalog [4], the OSACA catalog currently includes only these stars, although we collect data for other stars in our database as well. The proper motions of the HIPPARCOS stars considered have median errors in the proper motion of $\pm 0.0007''\,\mathrm{yr}^{-1}$, in the right ascension and declination of $\pm 0.0006''\,\mathrm{yr}^{-1}$, and in the tangential velocity of $\pm 0.0009''\,\mathrm{yr}^{-1}$. The proper motions of some of the stars considered have low accuracy due to their binarity. To refine these proper motions, we used a combination of coordinate and proper-motion data from the HIPPARCOS catalog and from ground-based catalogs in accordance with the method of Goncharov and Kiyaeva [5]. The parallaxes, equatorial coordinates, and proper motions of the stars considered are updated comparatively infrequently, when new data whose accuracy are superior to the HIPPARCOS data become available. Thus, the main data that are collected and refined are the stellar radial velocities.

Table 2. Format of the current release of the OSACA catalog

HIPPARCOS number	I6
Right ascension in decimal degrees	F11.6
Declination in decimal degrees	F11.6
Parallax in milliarcseconds	F7.2
Standard error of the parallax in milliarcseconds	F7.2
Fractional error of the parallax	F6.2
Decimal logarithm of the parallax in milliarcseconds	F6.2
Proper motion in the right ascension in $0.001''\,\mathrm{yr}^{-1}$	F9.1
Standard error of the proper motion in the right ascension in $0.001''\,\mathrm{yr}^{-1}$	F6.1
Proper motion in the declination in $0.001''\,\mathrm{yr}^{-1}$	F9.1
Standard error of the proper motion in the declination in $0.001''\,\mathrm{yr}^{-1}$	F6.1
Radial velocity in $\mathrm{km\,s}^{-1}$	F7.1
Standard error of the radial velocity in $\mathrm{km\,s}^{-1}$	F4.1
V magnitude in the Johnson system (from HIPPARCOS)	F6.2
B magnitude in the Johnson system (from HIPPARCOS)	F6.2
I magnitude in the Johnson system (from HIPPARCOS)	F6.2
$B-V$ color index in the Johnson system (from HIPPARCOS)	F7.3
$V-I$ color index in the Johnson system (from HIPPARCOS)	F6.2
Interstellar extinction A_v [6]	F5.2
Absolute magnitude M_V	F6.1
Binarity parameter: 1—single star, 2—nonsingle star	A1
Spectral type and luminosity class (from HIC [7])	A13
Galactic longitude in decimal degrees	F11.6
Galactic latitude in decimal degrees	F11.6
Proper motion in the Galactic longitude in $0.001''\,\mathrm{yr}^{-1}$	F8.1
Proper motion in the Galactic latitude in $0.001''\,\mathrm{yr}^{-1}$	F8.1
Total space velocity in $\mathrm{km\,s}^{-1}$	F7.1
Velocity component U in the Galactic coordinate system in $\mathrm{km\,s}^{-1}$	F8.1
Velocity component V in the Galactic coordinate system in $\mathrm{km\,s}^{-1}$	F8.1
Velocity component W in the Galactic coordinate system in $\mathrm{km\,s}^{-1}$	F8.1
X coordinate in the Galactic coordinate system in pc	F8.1
Y coordinate in the Galactic coordinate system in pc	F8.1
Z coordinate in the Galactic coordinate system in pc	F8.1

The catalog currently includes the main table, a table of references to published radial velocities (one line per star), a table of references to published radial velocities (one line per publication), and a table of cross identifications of the stars. Table 2 gives the format of the main table of the current release of the catalog. Figure 1 shows the distribution of the stars in absolute magnitude and heliocentric distance for single (solid) and multiple (dashed) stars. The

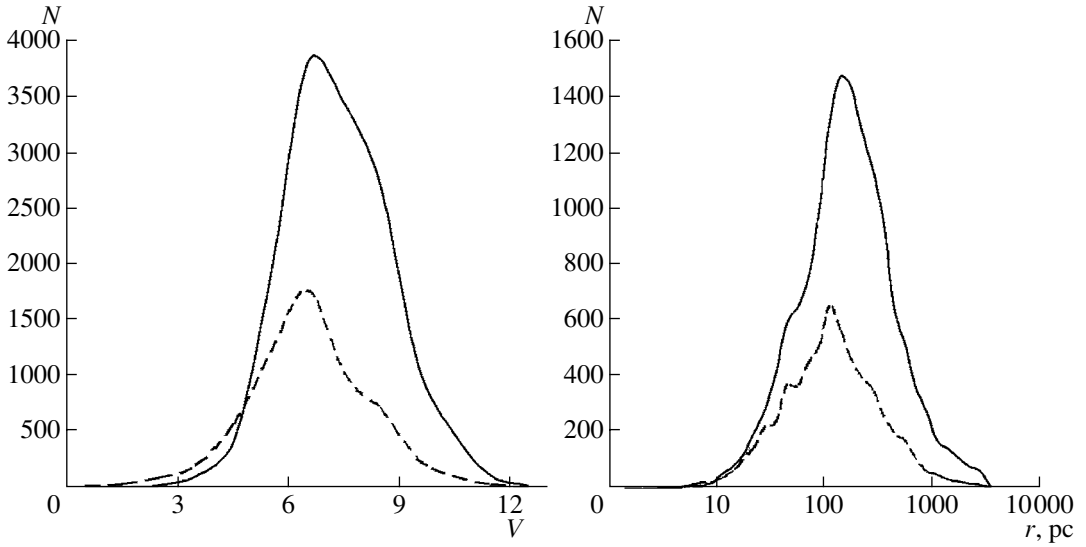

Fig. 1. Distributions of OSACA stars in absolute magnitude and heliocentric velocity for single (solid) and multiple (dashed) stars.

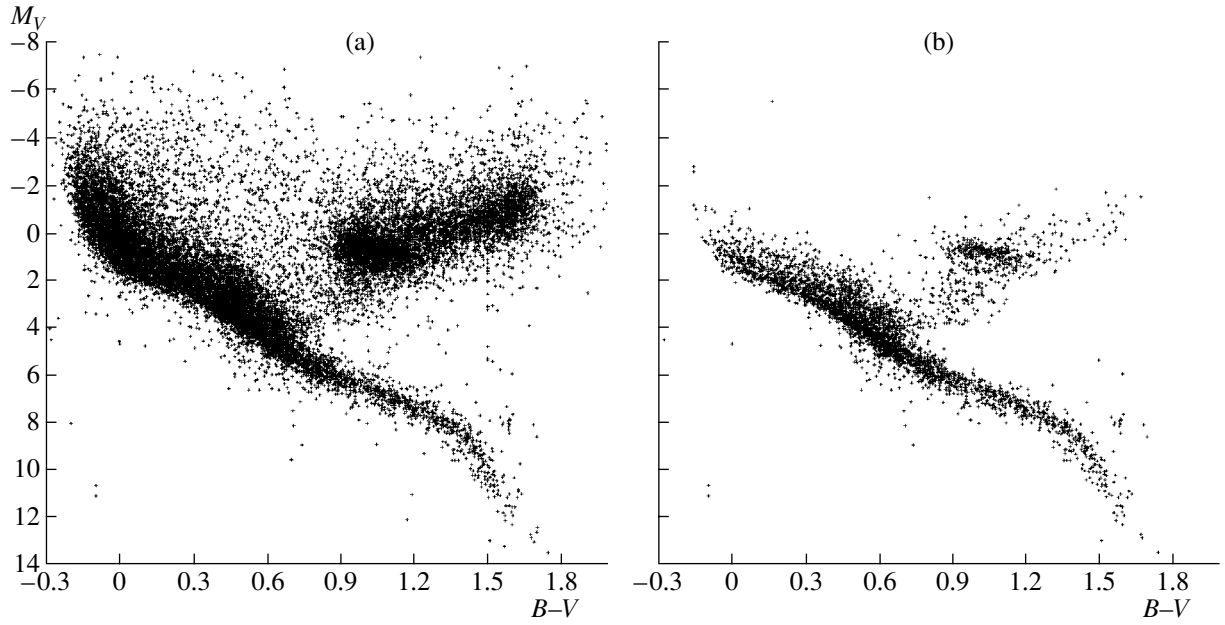

Fig. 2. Distributions of OSACA stars in the $(B-V)-M_V$ color-magnitude diagram for (a) all the stars and (b) single stars closer than 0.1 kpc.

distribution of the stars in the absolute magnitude–$B-V$ color index diagram (Fig. 2) resembles the corresponding distribution for all the stars of the HIPPARCOS catalog—all spectral types and luminosity classes are represented.

3. CALCULATION OF THE RADIAL VELOCITIES

The WEB catalog [8] contains about 14 300 HIPPARCOS stars with precise parallaxes and radial velocities known to better than ± 5 km s^{-1}. The catalog of Barbier-Brossat and Figon [9] contains about 16 000 such stars. Our catalog contains more than 28 000 such stars, reflecting the large number of high-precision radial-velocity measurements obtained in recent years, including the measurements for more than 10 000 stars reported in the CORAVEL–CfA catalog, as well as our reduction of all the radial-velocity catalogs employed to a single system.

We calculated the weighted mean radial velocities using data from more than 1400 publications. The full list of these sources can be found on the OSACA web page (http://www.geocities.com/orionspiral/). Examples of extensive catalogs that we employed include [10–21] and all the sources used to produce the catalogs [8, 9, 22]. All the sources of the radial velocities can be subdivided into two parts: (1) about one hundred major source catalogs, each of which usually has its own system of radial velocities, and (2) over one thousand publications dedicated to individual stars or small groups of stars. In the former case, the systematic errors for a particular catalog can be revealed by comparing it to some standard or other catalog, whereas such a comparison is impossible in the latter case due to the small number of stars. If individual observations of stars were made with the same instrument as the measurements reported in some major catalog, we can hope that the radial-velocity system will be the same for these observations, so that the systematic corrections assigned to the instrument in question can be applied to that individual star.

The problem of radial-velocity standards has a long history and has become especially topical in recent years (see, e.g., [23–27]). At present, only 181 stars approved by the International Astronomical Union (IAU) as radial-velocity standards have been confirmed to have constant radial velocities. The HD and HIPPARCOS numbers, radial velocities, V magnitudes and absolute magnitudes, and $B-V$ color indices of these stars are given in the table posted on the OSACA web page; in these cases, the "source" column indicates "IAU."

However, the need to use certain stars as radial-velocity standards has been questioned in recent years due to the emergence of astrometric methods of measuring radial velocities [16] and the fundamental possibility of calibrating an instrument by observing the radial velocities of Solar-system bodies.

Nidever et al. [27] (which we will refer to as the Keck catalog) shows that (1) the use of standard stars and solar system bodies yields virtually the same radial velocities to within ± 0.5 km s^{-1}; (2) it is possible to create a list of several hundred standard stars for determining radial velocities with errors no greater than ± 0.5 km s^{-1}, which would reasonably represent the entire variety of spectral types, luminosity classes, and other stellar parameters; and (3) determining the *absolute* radial velocities to better than ± 0.5 km s^{-1} requires allowance for numerous effects that thus far lack a sufficient theoretical basis (to say nothing of the procedures for taking them into account in practice).

Stellar kinematic studies require not so much radial velocities with very high precision as a homogeneous data set of radial velocities for a large number of various stars. A precision of ± 1 km s^{-1} can be considered to be acceptable for such studies. A velocity of 1 km s^{-1} corresponds to 1 pc Myr^{-1}. This precision enables the calculation of Galactic orbits and the analysis of the evolution of Galactic structures and groups of stars within 500 pc of the Sun over several tens of million of years in the past and future. Moreover, within a large volume of space, a precision of ± 1 km s^{-1} is comparable to the median accuracy of stellar tangential velocities calculated from proper motions, namely, $\pm 0.001''$ yr^{-1}; within 200 pc of the Sun, the tangential velocities are, on average, known better than the corresponding radial velocities (for about two-thirds of all the stars considered), whereas the situation is reversed for more distant stars (about one-third of all the stars).

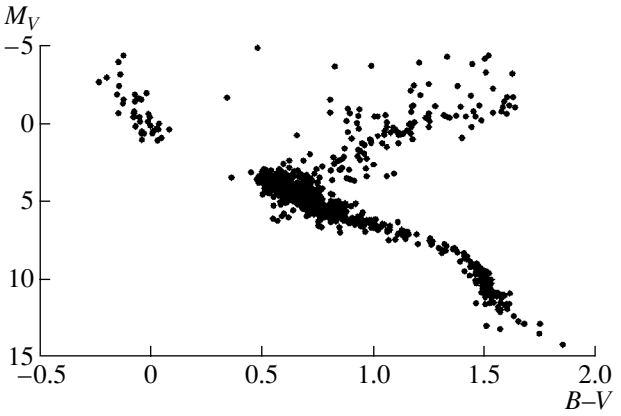

Fig. 3. $(B-V)-M_V$ color index–absolute magnitude diagram for IAU–Keck standard stars.

The Keck catalog includes a list of 782 stars proposed for use as standard stars for determinations of radial velocities. These stars have stable *relative* radial velocities and represent different types of stars; the radial velocities of IAU standard stars in the Keck catalog agree with the standard radial velocities to within no worse than ± 0.5 km s^{-1}. Although some of these stars exhibited radial-velocity variations after the release of the Keck catalog, the overwhelming majority can be adopted as supplementary standards for the determination of radial velocities with a precision of $\pm(0.5-1)$ km s^{-1}. The parameters of 673 such stars with Keck indicated in the source column are given in the table posted on the OSACA web page.

The full list of 854 standard stars that we used to transform more than 50 000 published radial velocities into a single standard system that we refer to as the IAU–Keck system does not include some stars in the initial IAU and Keck lists that have exhibited appreciable radial-velocity variations in recent years. Figure 3 shows the distribution of these stars on the $(B-V)-M_V$ color index–absolute magnitude

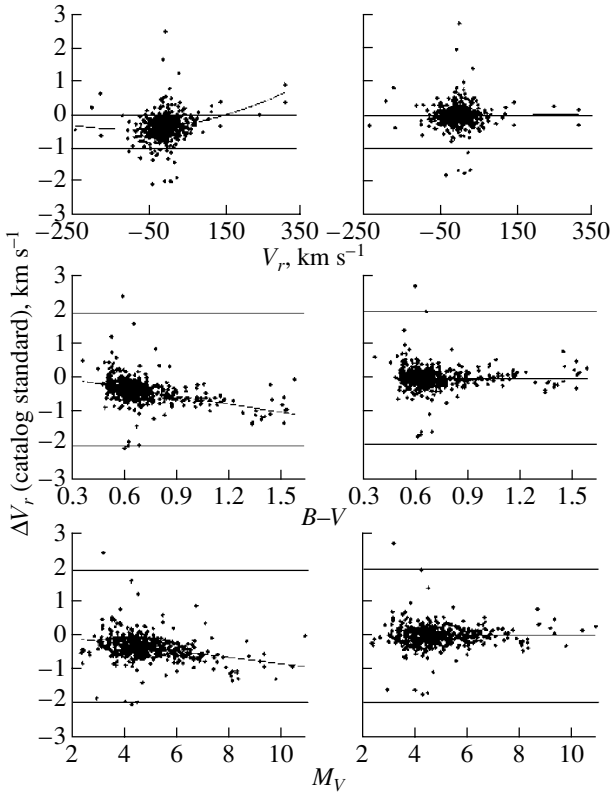

Fig. 4. CORAVEL–CfA minus the standard radial-velocity differences for 484 stars in common as a function of various parameters before (left-hand plots) and after (right-hand plots) allowance for systematic effects.

diagram. It is evident that types of stars that are not represented or under-represented include white dwarfs, subdwarfs, subgiants, and A5 to F5 main-sequence stars.

The transformation of a published radial-velocity catalog into the standard system involves the calculation of "catalog minus standard" differences for stars in common followed by the identification and approximation of systematic dependences of these differences on various stellar parameters allowing the systematic differences identified to be eliminated for all stars.

As an example, let us consider the systematic errors that we revealed for the CORAVEL–CfA catalog. Figure 4 shows the dependences of the radial-velocity differences in the sense "CORAVEL–CfA minus standard" for 484 stars in common as a function of the radial velocity, $B-V$ color index, and absolute magnitude (we also found the dependences on the effective temperature, H_β index, and metallicity Fe/H). The left- and right-hand plots show the data before and after elimination of the following dependences:

$$\Delta V_r = -0.8398(B-V) + 0.2531,$$

$$\Delta V_r = 0.000008V_r^2 + 0.0012V_r - 0.0142,$$

where ΔV_r is the difference of the radial velocities for stars in common in the sense of CORAVEL–CfA minus the standard, $B-V$ is the color index, and V_r is the radial velocity. It is obvious from these plots that eliminating the dependences on the radial velocity and $B-V$ color index also eliminated the dependence on the absolute magnitude (and on other parameters as well); no new dependences appeared in the process, and the standard deviation of the CORAVEL–CfA minus the standard radial-velocity differences decreased from 0.38 to 0.33 km s^{-1} for the stars in common. This quantity can be viewed as an approximate estimate of the systematic accuracy of the CORAVEL–CfA catalog.

We used the same procedure to bring other catalogs to the IAU–Keck standard system. As for the stars of the CORAVEL–CfA catalog, the most widespread systematic errors for these stars depend on the radial velocity and $B-V$. Dependences on these two parameters are usually manifest in observations of radial velocities (see, e.g., [27]).

After transforming all the radial velocities to the single system, we calculate for each star its weighted mean radial velocity. In this case, we set the weights in accordance with the standard deviation of the catalog minus standard radial-velocity differences for stars in common to the catalog and standard. We assign single observations the same weight as that for catalogs obtained from observations performed with the same instrument.

The radial velocities of the CORAVEL–CfA catalog transformed to the standard IAU–Keck system have such high precisions compared to many other sources and the CORAVEL–CfA catalog has such high weights that the weighted mean velocities for these stars barely differ from the corresponding CORAVEL–CfA radial velocities with the systematic errors corrected.

However, some of the CORAVEL–CfA data should be treated with caution. Figure 5 compares the radial velocities and U, V, W space-velocity components from the CORAVEL–CfA catalog and from our calculations based on two other sources of radial velocities for 3400 stars in common (all radial velocities were transformed to a single system and the same HIPPARCOS/Tycho-2 proper motions were used). All the quantities are appreciably correlated. The differences in the radial velocities are due mostly to errors in catalogs that are less accurate than the CORAVEL–CfA catalog. However, a fairly large number of stars exhibit discrepances between the U, V, and W values from the CORAVEL–CfA catalog and our calculations. This discrepancy is due to the distances employed: we used distances calculated from the HIPPARCOS trigonometric parallaxes, whereas photometric parallaxes were used

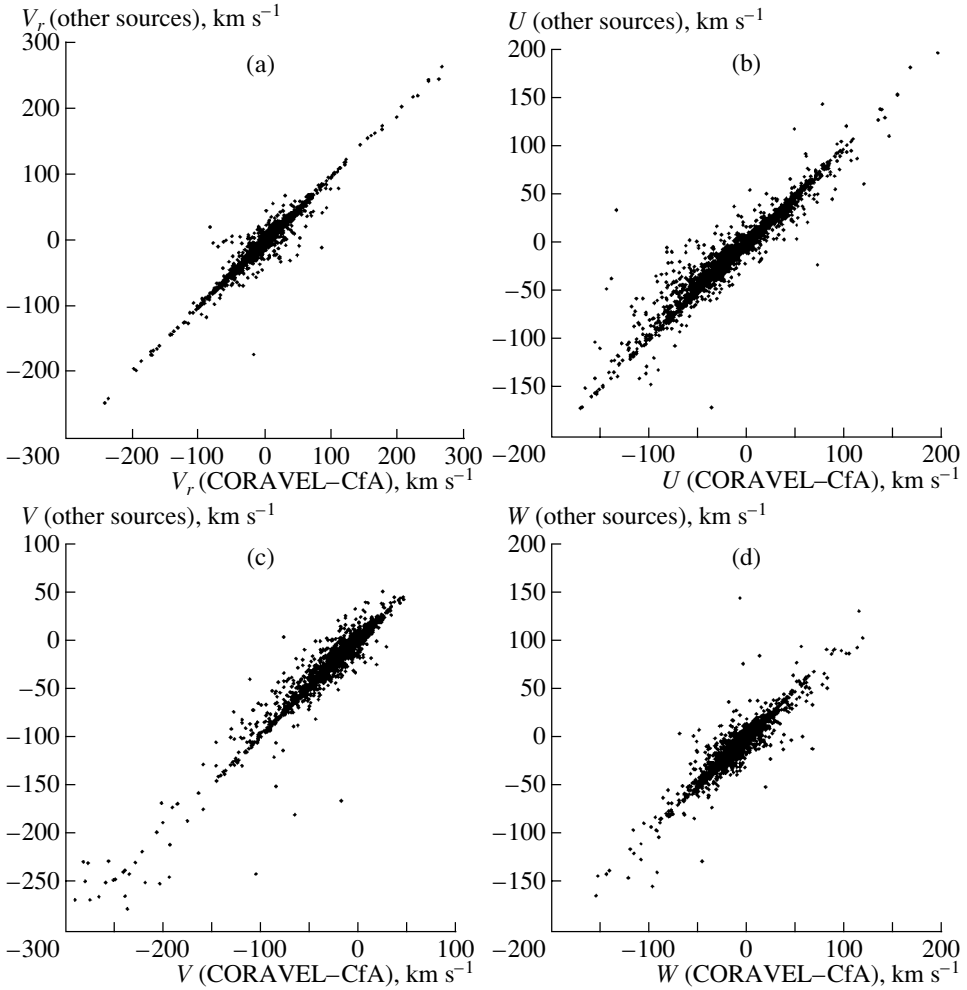

Fig. 5. Comparison of the (a) radial velocities, (b) U velocity components, (c) V velocity components, and (d) W velocity components from the CORAVEL–CfA catalog with the corresponding velocities calculated from other radial-velocity sources (for a total of 3400 stars in common).

to calculate the distances in the CORAVEL–CfA catalog and the corresponding factor for transforming the proper motions into linear velocities for stars for which the relative errors of the HIPPARCOS parallaxes is greater than 13%. The authors of the CORAVEL–CfA catalog admit that these photometric parallaxes are not suitable for binary stars, giants, and several other categories of stars. We found most of the stars with fairly discordant U, V, and W velocity components for the CORAVEL–CfA catalog and our own data, indeed, to be such "problematic" objects, whose photometric parallaxes in the CORAVEL–CfA catalog are systematically greater than the corresponding trigonometric parallaxes (and whose heliocentric distances are systematically smaller). As is evident from Fig. 6, the same effect arises for the same "problem" stars when we compare the distances based on the HIPPARCOS parallaxes and the CORAVEL–CfA distances and in the appreciable difference between our absolute magnitudes and the absolute magnitudes adopted from the CORAVEL–CfA catalog (note that the discrepancy between the interstellar extinctions inferred using different methods is insignificant, since we are dealing with fairly nearby stars whose extinction does not, on average, exceed 0.1^m).

Among the stars considered here are more than 7000 known or suspected multiple stars, including more than 800 known and 4500 suspected spectral binaries. Therefore, one of the problems we had to face when calculating the weighted mean radial velocities were the errors in the identification of components of multiple systems made in many publications. In other words, authors often incorrectly identify the component whose radial velocity they have measured or even fail to mention the component to which the measurement refers. These errors are largely due to the the fact that, until recently, the nomenclature for

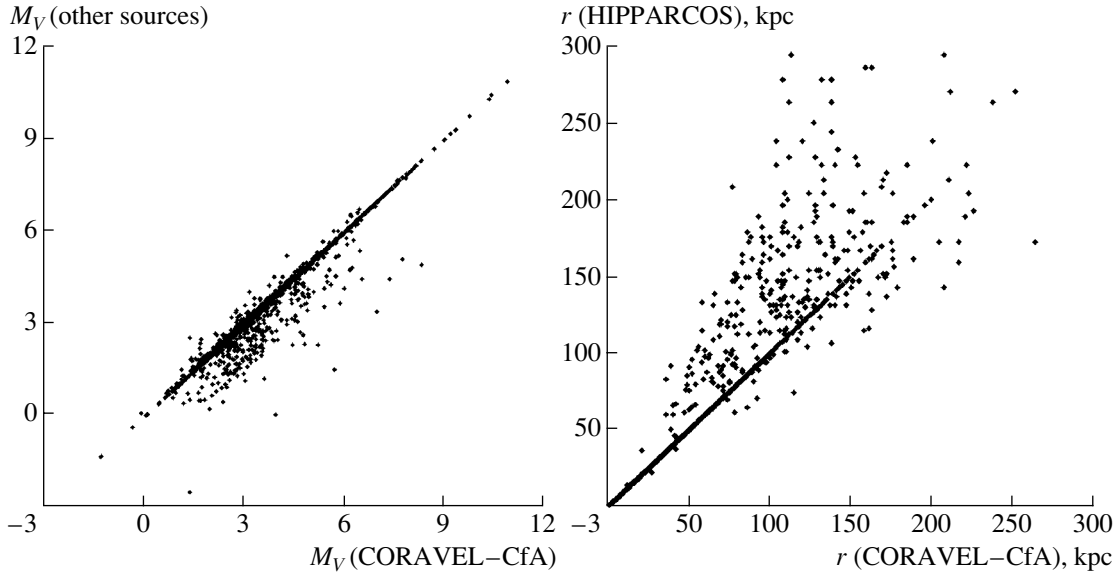

Fig. 6. Left: comparison of absolute magnitudes from the CORAVEL–CfA catalog with the absolute magnitudes calculated from the HIPPARCOS parallaxes with allowance for interstellar extinction (3400 stars in common). The difference is due to the differences in the allowance for extinction and the use of inaccurate photometric parallaxes in the CORAVEL–CfA catalog. Right: heliocentric distances of stars of the CORAVEL–CfA catalog compared to their heliocentric distances from the HIPPARCOS catalog.

stellar and planetary systems was not standardized; i.e., the same component had different designations in different catalogs. We made a number of corrections of this type.

In all the cases where there is no doubt that the components of a stellar system are gravitationally bound (the component separation does not exceed 20 000 AU), we calculated only the systemic radial velocities and will consider only these velocities further. In the case of gravitationally wide stellar pairs (with component separations exceeding 20 000 AU), the OSACA catalog lists all components with measured radial velocities.

Estimates of the errors in the radial velocities are available for most of the stars in the OSACA database, enabling us to estimate the random errors in the observed space velocities. For example, 26 492 stars satisfy the criteria

$$e_\pi/\pi < 0.3, \quad (1)$$

$$e_V < 15\ \mathrm{km\,s^{-1}}, \quad (2)$$

$$V_{pec} < 100\ \mathrm{km\,s^{-1}}. \quad (3)$$

Here, e_π/π is the fractional error in the parallax, $e_V = \sqrt{e_{V_r}^2 + e_{V_l}^2 + e_{V_b}^2}$ is the error in the observed velocity vector $V = (V_r, V_l, V_b)$, where V_r is the radial component of the velocity, $V_l = 4.74\mu_l \cos b r$ is the velocity component in the direction of the Galactic longitude, and $V_b = 4.74\mu_b r$ is the velocity component in the direction of the Galactic latitude; $V_{pec} = \sqrt{U^2 + V^2 + W^2}$ is the residual (particular) velocity of the star relative to the local standard of rest. We estimated the errors in V_l and V_b taking into account the errors in the parallax but without allowance for correlations between the proper-motion components $\mu_l \cos b$ and μ_b, using the formula

$$e_{(V_l,V_b)} = \frac{4.74}{\pi}\sqrt{\mu_{l,b}^2\left(\frac{e_\pi}{\pi}\right)^2 + e_{\mu_{l,b}}^2},$$

where $\mu_{l,b}$ are the tangential-velocity components. We set the velocity of the Sun relative to the local standard of rest equal to $(u_\odot, v_\odot, w_\odot) = (10.0, 5.3, 7.2)\ \mathrm{km\,s^{-1}}$, in accordance with [28]. We found the mean random errors to be $\bar{e}_{V_r} = 2.7\ \mathrm{km\,s^{-1}}$, $\bar{e}_{V_l} = 2.3\ \mathrm{km\,s^{-1}}$, and $\bar{e}_{V_b} = 1.7\ \mathrm{km\,s^{-1}}$.

4. METHODS FOR THE KINEMATIC ANALYSIS

In this paper, we analyze the kinematics of stars based on the OSACA catalog in an Ogorodnikov–Milne model. We analyze the residual velocities using the classic method of determining the Schwarzschild ellipsoid and two-dimensional distributions of the U, V velocity components.

4.1. The Ogorodnikov–Milne Model

We used a linear Ogorodnikov–Milne model with the notation introduced by Clube [29, 30]. The ob-

served velocity $\mathbf{V}(r)$ of a star with a heliocentric radius vector $\mathbf{r}$ can be described by the following vector equation, up to the first-order in the small quantity $r/R_\circ \ll 1$:

$$\mathbf{V}(r) = \mathbf{u}_\circ + M\mathbf{r} + \mathbf{V}',$$

where $\mathbf{u}_\circ$ is the velocity of the centroid of the stars relative to the Sun $(-V_\odot(u_\odot, v_\odot, w_\odot))$; $\mathbf{V}$ is the residual velocity of the star (here we assume that the stellar residual velocities are randomly distributed); and M is the matrix (tensor) of the displacements, whose components are equal to the partial derivatives of $\mathbf{u}(u_1, u_2, u_3)$ with respect to $\mathbf{r}(r_1, r_2, r_3)$:

$$M_{pq} = \left(\frac{\partial u_p}{\partial r_q}\right)_\circ, \quad p, q = 1, 2, 3.$$

The matrix M can be decomposed into the local-deformation tensor M^+ and the local-rotation tensor M^- [31]:

$$M^+_{pq} = \frac{1}{2}\left(\frac{\partial u_p}{\partial r_q} + \frac{\partial u_q}{\partial r_p}\right)_\circ, \tag{4}$$

$$M^-_{pq} = \frac{1}{2}\left(\frac{\partial u_p}{\partial r_q} - \frac{\partial u_q}{\partial r_p}\right)_\circ, \quad p, q = 1, 2, 3.$$

The working equations have the form

$$V_r = f(u_\odot, v_\odot, w_\odot, M_{11}, \ldots, M_{33}), \tag{5}$$

$$V_l = f(u_\odot, v_\odot, M_{11}, \ldots, M_{23}), \tag{6}$$

$$V_b = f(u_\odot, v_\odot, w_\odot, M_{11}, \ldots, M_{33}) \tag{7}$$

(see [32] for more details). The set of conditional equations (5)–(7) contains 12 unknowns: three velocity components for $V_\odot$ and nine components of M_{pg}, which are estimated using the least-squares method. We then calculate the components of the deformation and rotation tensors using the already derived M_{pq} values based on (4). Thus, the Oort constants can be calculated as follows: $A = 0.5(M_{12} + M_{21})$, $B = 0.5(M_{21} - M_{12})$, $C = 0.5(M_{11} - M_{22})$, and $K = 0.5(M_{11} + M_{22})$, and the vertex deviation l_{xy} can be calculated from the formula $\tan 2l_{xy} = -C/A$. The angular velocity of the Galactic rotation can be obtained from the formulas $\omega_\circ = B - A = -M_{12}$. The form of these equations is such that negative $\omega_\circ$ corresponds to the direction of the Galactic rotation.

4.2. Determination of the Schwarzschild Ellipsoid

We calculated the elements of the residual-velocity ellipsoid (Schwarzschild ellipsoid) using the well-known statistical method described in detail in [31, 33, 34]. This method consists in determining the symmetric momentum tensor. We have six equations for each star that can be used to determine the six unknown components of the velocity-dispersion tensor. Analysis of the eigenvalues of the velocity-dispersion tensor yields the principal semiaxes $\sigma_{1,2,3}$ of the residual-velocity ellipsoid $\sigma_{1,2,3}$ and also the directions $l_{1,2,3}$, $b_{1,2,3}$ of the principal axes. When writing the formulas for the stellar residual velocities, we take into account the overall rotation of the Galaxy by adopting the Oort constants $A = 13.7\ \mathrm{km\,s^{-1}\ kpc^{-1}}$ and $B = -12.9\ \mathrm{km\,s^{-1}\ kpc^{-1}}$, in accordance with [35].

4.3. Two-Dimensional Maps of the Space Velocities

It is of interest to construct and analyze two-dimensional velocity maps, in particular, velocity maps in the U, V plane [36, 37], in order to analyze the fine structure of the distributions of the residual space velocities in order to identify clusters, streams, etc. We estimated the two-dimensional probability density $f(U, V)$ from the calculated, discretely distributed U, V velocities using the method of adaptive smoothing [36] with a two-dimensional radially symmetric Gaussian kernel:

$$K(r) = \frac{1}{\sqrt{2\pi}\sigma}\exp\left(-\frac{r^2}{\sigma^2}\right),$$

where $r^2 = x^2 + y^2$. In this case, the necessary relation $\int K(r)dr = 1$ for the probability density estimates is satisfied. The main idea behind this method is that, at each point of the map, smoothing is performed by a beam whose size is determined by a parameter σ, which varies depending on the data in the neighborhood of the point considered. Thus, the smoothing is performed using a fairly narrow beam in high-density regions, and the beam width increases with decreasing density. We use the following definition for adaptive smoothing at an arbitrary point $\xi = (U, V)$ [36]:

$$\hat{f}(\xi) = \frac{1}{n}\sum_{i=1}^{n} K\left(\frac{\xi - \xi_i}{h\lambda_i}\right),$$

where $\xi_i = (U_i, V_i)$, λ_i is a local dimensionless parameter of the beam at the point ξ_i, h is a general smoothing parameter, and n is the number of data points $\xi_i = (U_i, V_i)$. The parameter λ_i at each point of the two-dimensional U, V plane is defined as follows:

$$\lambda_i = \sqrt{\frac{g}{\hat{f}(\xi)}}, \quad \ln g = \frac{1}{n}\sum_{i=1}^{n}\ln\hat{f}(\xi),$$

where g is the geometric mean $\hat{f}(\xi)$. It is evident that, to determine λ_i, we must know the distribution $\hat{f}(\xi)$, which, in turn, can be determined if all λ_i are known. Therefore, the problem of finding the unknown distribution must be solved iteratively. As a

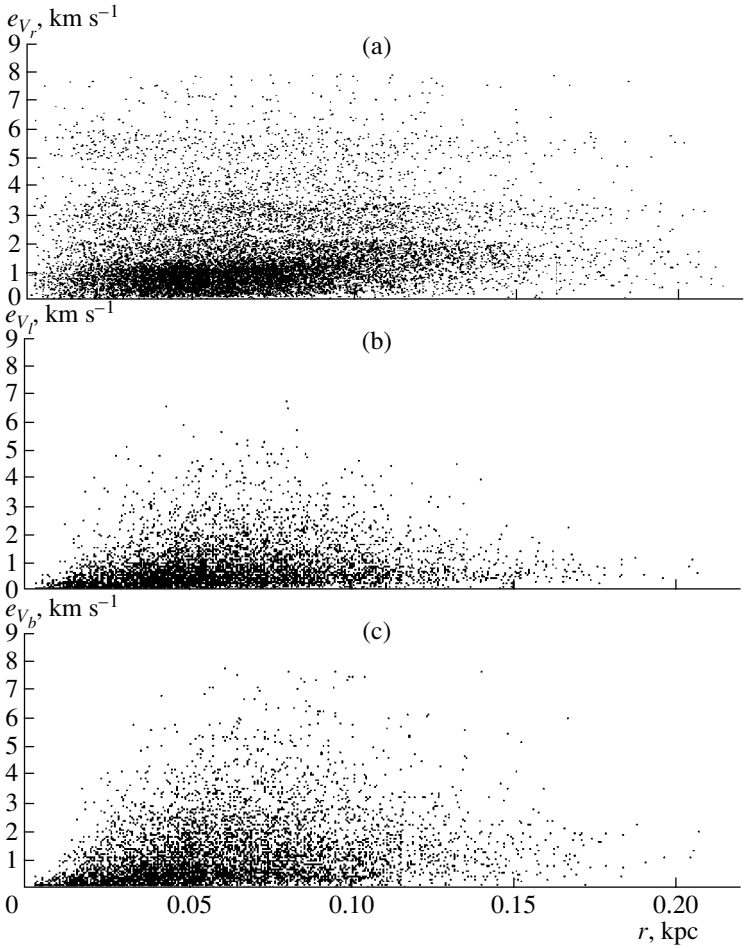

Fig. 7. Random errors of the velocities of nearby main-sequence stars as a function of the heliocentric distance.

first approximation, we use the distribution obtained by smoothing the initial U, V map with a fixed-sized beam. The optimum value of the parameter h can be determined by minimizing the mean square deviation of the estimate $\hat{f}(\xi)$ from the true distribution $f(\xi)$. The h values that we inferred for the various stellar samples considered here vary from 6 to 10 km s^{-1}. A typical uncertainty in the velocity is 2 km s^{-1} in this case. This influenced our choice of the discretization interval for the two-dimensional maps; the area of a square pixel was taken to be $S = 2 \times 2$ km^2 s^{-2}. The map must be scaled using the factor nS.

5. RESULTS OF THE KINEMATIC ANALYSIS

5.1. Effect of Binary Stars

The aim of this section is to establish how the binarity of stars affects the parameters of the Ogorodnikov–Milne model. To identify possible features that depend on the stellar age, we selected from the OSACA catalog stars of luminosity classes V and IV, i.e., main-sequence stars satisfying the conditions

$$e_\pi/\pi < 0.1, \quad e_V < 8 \text{ km s}^{-1},$$

and also condition (3). Figure 7 shows the distribution of random errors of the V_r, V_l, V_b components of the observed space velocities as a function of distance for the resulting sample of 6276 stars. We find the mean random errors of the velocity components to be $\bar{e}_{V_r} = 1.1$ km s^{-1}, $\bar{e}_{V_l} = 1.3$ km s^{-1}, $\bar{e}_{V_b} = 0.9$ km s^{-1}. In this case, the mean error in the absolute space velocity is 1.9 km/s. The homogeneous nature of our data enables us to solve the initial equations (5)–(7) with unit weights.

We first subdivided the entire sample into two parts depending on the color index, with the boundary at $B-V = 0.5$, then produced for each part subsamples consisting of either single or binary stars. Table 3 gives our derived components of the solar velocity, $V_\odot(u_\odot, v_\odot, w_\odot)$ relative to the corresponding stellar centroid, the coordinates $L_\odot$ and $B_\odot$ of the apex of the solar motion, the elements M_{pq} of the displacement tensor and roots $\lambda_{1,2,3}$ of the deformation tensor, the

Table 3. Kinematic parameters of nearby main-sequence stars

Parameter	Single stars	Binary stars	Single stars	Binary stars
	$B-V \le 0.5$		$B-V > 0.5$	
	$N_\star = 1720$ $\bar{r} = 67$ pc	$N_\star = 1100$ $\bar{r} = 51$ pc	$N_\star = 2318$ $\bar{r} = 39$ pc	$N_\star = 1138$ $\bar{r} = 30$ pc
$u_\odot$, km s^{-1}	10.8 ± 0.4	10.4 ± 0.5	9.0 ± 0.6	10.8 ± 0.9
$v_\odot$, km s^{-1}	11.8 ± 0.4	11.8 ± 0.5	20.2 ± 0.6	21.9 ± 0.9
$w_\odot$, km s^{-1}	6.9 ± 0.4	7.3 ± 0.5	8.1 ± 0.6	7.4 ± 0.9
$V_\odot$, km s^{-1}	17.4 ± 0.4	17.3 ± 0.5	23.5 ± 0.6	25.5 ± 0.9
$L_\odot$, deg	48 ± 1	48 ± 2	66 ± 2	64 ± 2
$B_\odot$, deg	24 ± 1	25 ± 2	20 ± 2	17 ± 2
M_{11}, km s^{-1} kpc^{-1}	-12 ± 9	11 ± 12	-21 ± 18	103 ± 29
M_{12}, km s^{-1} kpc^{-1}	52 ± 7	33 ± 9	103 ± 17	27 ± 25
M_{13}, km s^{-1} kpc^{-1}	-16 ± 9	-3 ± 12	-22 ± 17	0 ± 28
M_{21}, km s^{-1} kpc^{-1}	-7 ± 9	-25 ± 12	2 ± 18	51 ± 29
M_{22}, km s^{-1} kpc^{-1}	19 ± 7	10 ± 9	20 ± 17	7 ± 25
M_{23}, km s^{-1} kpc^{-1}	4 ± 9	28 ± 12	15 ± 17	-16 ± 28
M_{31}, km s^{-1} kpc^{-1}	2 ± 9	-9 ± 12	16 ± 18	1 ± 29
M_{32}, km s^{-1} kpc^{-1}	3 ± 7	4 ± 9	-28 ± 17	19 ± 25
M_{33}, km s^{-1} kpc^{-1}	6 ± 9	-10 ± 12	0 ± 17	-15 ± 28
λ_1, km s^{-1} kpc^{-1}	31 ± 9	19 ± 12	57 ± 18	117 ± 29
λ_2, km s^{-1} kpc^{-1}	-25 ± 9	-21 ± 12	-57 ± 18	-15 ± 29
λ_3, km s^{-1} kpc^{-1}	8 ± 9	13 ± 12	-1 ± 17	-7 ± 28
σ_1, km s^{-1}	23.09 ± 0.55	22.67 ± 0.67	33.84 ± 0.76	33.82 ± 1.07
σ_2, km s^{-1}	13.21 ± 0.52	13.20 ± 0.59	22.00 ± 0.52	23.06 ± 0.73
σ_3, km s^{-1}	10.15 ± 0.37	10.21 ± 0.45	17.75 ± 0.41	17.27 ± 0.56
$l_1,\ b_1$, deg	$14 \pm 3, -1 \pm 0$	$15 \pm 11, -2 \pm 2$	$8 \pm 1, 0 \pm 0$	$9 \pm 9, -2 \pm 2$
$l_2,\ b_2$, deg	$104 \pm 2, 0 \pm 1$	$105 \pm 3, 4 \pm 2$	$98 \pm 2, 5 \pm 1$	$98 \pm 4, 9 \pm 2$
$l_3,\ b_3$, deg	$349 \pm 2, 89 \pm 6$	$315 \pm 3, 86 \pm 5$	$275 \pm 2, 86 \pm 5$	$291 \pm 4, 81 \pm 5$

principal axes $\sigma_{1,2,3}$ of the residual-velocity ellipsoid, and the directions $l_{1,2,3}$, $b_{1,2,3}$ of the principal axes. As is evident from the upper part of the table, the components of the solar motion based on the samples of single and binary stars do not differ significantly in any of the color intervals.

The only elements of the displacement tensor to differ significantly from zero are M_{12} for the three samples indicated in columns 2–4 and M_{11} for the last sample of binary main-sequence red dwarfs (column 5). The M_{11} values derived for the samples of single and binary red dwarfs differ by $\Delta M_{11}\bar{r} \approx 3 \pm 1$ km s^{-1}.

Two roots of the deformation tensor, $\lambda_{1,2}$, differ significantly from zero for the two single-star samples (columns 2 and 4), whereas the third root, λ_3, does not differ significantly from zero. Hence, we have a planar case where $\lambda_{(1,2)} = K \pm \sqrt{A^2 + C^2}$ [38]. The closeness of the absolute values of the roots λ_1 and λ_2 is suggestive of rotation (without expansion/contraction).

The deformation tensor for the binary red dwarfs represents a linear case with a single significant root

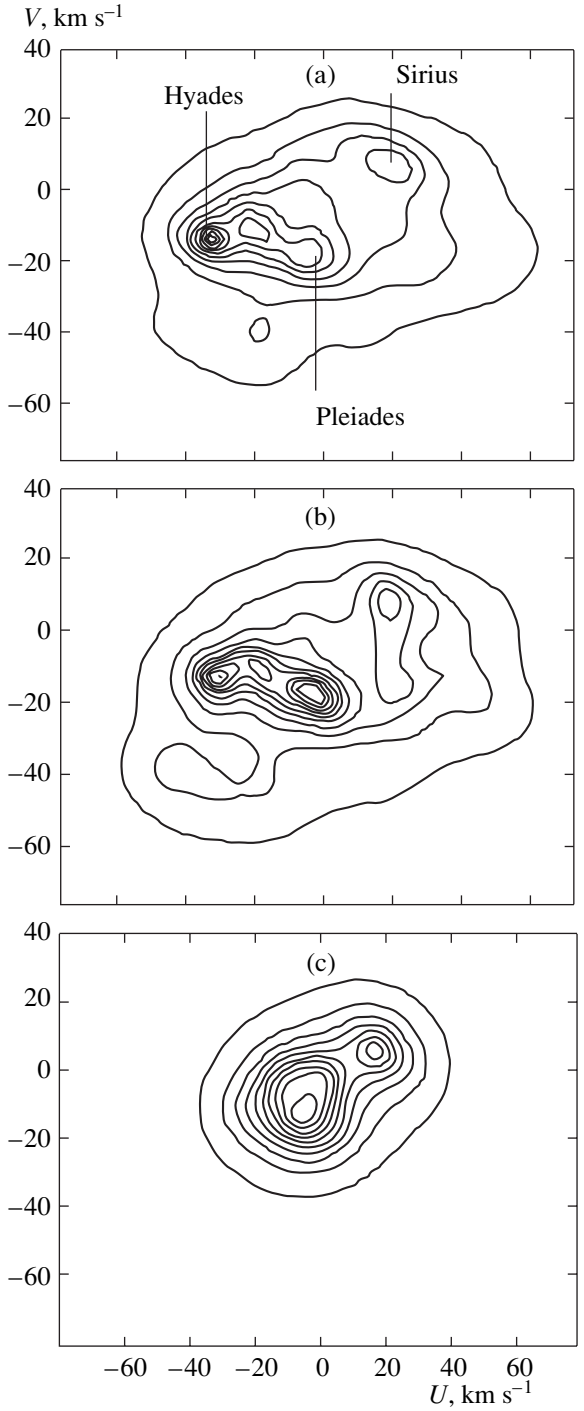

Fig. 8. Distributions of U and V (relative to the local standard of rest) for (a) single stars, (b) nearby main-sequence binaries with $(B-V > 0.5)$, and (c) stars with a negative K effect.

of $\lambda_1 = 117 \pm 29$ km s^{-1} kpc^{-1} and with the fairly high value $K = 55 \pm 19$ km s^{-1} kpc^{-1}. In this case, the ellipse of the deformation tensor is highly elongated along the x axis, i.e., we have expansion along a single axis.

As is evident from Table 3, the elements of the residual-velocity ellipsoids derived for the single and binary samples do not differ significantly in any of the color intervals. The elements of the residual-velocity ellipsoid derived for the binary stars have larger random errors.

The samples considered are the most refined in terms of the errors of the heliocentric distances and velocity components of the stars.

Our distributions of U, V (Fig. 8) show that the binary stars are much more concentrated than the single stars (by about a factor of two) near the local peaks associated with the Hyades and Pleiades clusters. Note that the bottom contour and contour step in the figures shown are 10% of the maximum value.

The specific features of the parameters of the Ogorodnikov–Milne model found by analyzing the samples of single and binary red dwarfs, such as the statistical significance of M_{11}, are consistent with our results based on an analysis of a significantly smaller sample of nearby visual binaries [39]. Note that we have determined the kinematic parameters with much higher precision in this current work. The distributions of the U, V velocities of both the single and multiple stars (Fig. 8), and of the red dwarfs (the oldest stars), in particular, show that star formation in the Galactic disk is influenced by some persistent factor, which could be associated with the bar at the Galactic center [40, 41] and/or the spiral structure of the Galaxy [42].

5.2. Negative K effect

The aim of this section is to analyze stars exhibiting the strongest negative K effect. To this end, we selected only single stars that obey relations (1)–(3) and the criterion $\pi < 10$ milliarcsec, which leaves us mostly with giants. All the selected stars are located at distances of 0.1–0.6 kpc. Our analysis of 9468 stars ($\bar{r} = 0.175$ kpc) of mixed spectral composition yielded $A = 12.3 \pm 1.0$ km s^{-1} kpc^{-1}, $B = -13.4 \pm 1.0$ km s^{-1} kpc^{-1}, $C = -6.1 \pm 1.0$ km s^{-1} kpc^{-1}, and $K = -4.1 \pm 1.0$ km s^{-1} kpc^{-1}. We found the vertex deviation to be $l = 13° \pm 2°$ and the angular velocity of the Galactic rotation to be $\omega_\circ = -25.7 \pm 1.2$ km s^{-1} kpc^{-1}. The derived values of the Oort constants A, B, and $\omega_\circ$ are, on the whole, fairly consistent with the Galactic-rotation parameters obtained in various other studies based on much more distant stars than those used here [35, 43, 44]. At the same time, we found K to differ significantly from zero, which is of considerable interest. A negative K effect in the Ogorodnikov–Milne model means that the stellar system considered is in a state of contraction.

Several authors [35, 45] have found negative K effects of $-(1-6)$ km s^{-1} kpc^{-1} in the motion of OB stars (out to heliocentric distances of $\approx$4 kpc). The nature of this result is not entirely clear. Various hypotheses have been suggested: it could be an effect due to the specifics of the methods used to measure the stellar radial velocities [46], or a result of the influence of the bar in the center of the Galaxy [46], or the effect of the spiral structure [47, 48]. Fernández et al. [49] tried to eliminate the negative K effect by taking into account the spiral structure, but their attempt failed, and the negative K effect remained.

Note that the youngest and nearest OB stars exhibit a characteristic positive K effect [32, 49], and, therefore, we do not consider these stars here.

In this work, we succeeded in forming a sample of stars with a maximum negative K effect, which consists of 1269 stars with color indices $B-V \leq 0.2$. We did not use stars of luminosity classes V and IV or O and B stars, so that the sample in question contains only stars of spectral types A0–A5 and luminosity classes I, II, III. However, the bulk of the sample is made up of stars with no luminosity classes given in the OSACA catalog. We then analyzed the residual velocities of the stars corrected for the overall Galactic rotation (see Section 4.2). Our analysis yielded for the particular velocity of the Sun $u_\odot = 10.2 \pm 0.4$ km s^{-1}, $v_\odot = 10.9 \pm 0.4$ km s^{-1}, $w_\odot = 6.6 \pm 0.4$ km s^{-1}, $V_\odot = 16.4 \pm 0.4$ km s^{-1}, $L_\odot = 47^\circ \pm 2^\circ$, $B_\odot = 24^\circ \pm 2^\circ$, and for the components M^+ and M^- of the tensor M (in units of km s^{-1} kpc^{-1}) characterizing the residual kinematic effects

$$M = \begin{pmatrix} -28.0_{(3.2)} & -1.4_{(2.5)} & -0.2_{(4.1)} \\ -11.4_{(3.2)} & 1.9_{(2.5)} & 2.6_{(4.1)} \\ 0.3_{(3.2)} & 0.2_{(2.5)} & -3.3_{(4.1)} \end{pmatrix},$$

$$M^+ = \begin{pmatrix} -28.0_{(3.2)} & -6.4_{(2.0)} & 0.0_{(2.6)} \\ -6.4_{(2.0)} & 1.9_{(2.5)} & 1.4_{(2.4)} \\ 0.0_{(2.6)} & 1.4_{(2.4)} & -3.3_{(4.1)} \end{pmatrix},$$

$$M^- = \begin{pmatrix} 0 & 5.0_{(2.0)} & -0.2_{(2.6)} \\ -5.0_{(2.0)} & 0 & 1.2_{(2.4)} \\ 0.2_{(2.6)} & -1.2_{(2.4)} & 0 \end{pmatrix}.$$

The roots of the deformation tensor $(\lambda_1, \lambda_2, \lambda_3)$ are $(3.5, -29.3, -3.5)$ km s^{-1} kpc^{-1} with standard errors of $\approx$3 km s^{-1} kpc^{-1}. The directions of the principal axes of the deformation tensor are

$$L_1 = 282^\circ \pm 2^\circ, \quad B_1 = -12^\circ \pm 1^\circ,$$
$$L_2 = 12^\circ \pm 4^\circ, \quad B_2 = -1^\circ \pm 26^\circ,$$
$$L_3 = 285^\circ \pm 4^\circ, \quad B_3 = 79^\circ \pm 6^\circ.$$

The vertex deviation in the xy plane is $l_{xy} = -33^\circ \pm 4^\circ$; we also derived the parameters of the K effect: $K = 0.5(M_{11} + M_{22}) = -13.1 \pm 2.0$ km s^{-1} kpc^{-1}, and $C = 0.5(M_{11} - M_{22}) = -14.9 \pm 2.0$ km s^{-1} kpc^{-1}.

The rotation tensor, M^-, contains no elements that differ significantly from zero, leading us to conclude that the radial component is the dominant effect in the residual motions of the stars considered. In this case, we set one of the roots (λ_3) equal to zero and consider only the xy plane. Since $(\partial V_R/\partial R)_{R_\circ} = \lambda_1$, we have $(V_R/R)_{R_\circ} = \lambda_2$, where R is the unknown distance from the kinematic center. However, the relations

$$K + C = 4 \pm 3 \text{ km s}^{-1} \text{ kpc}^{-1},$$
$$K - C = -29 \pm 3 \text{ km s}^{-1} \text{ kpc}^{-1}$$

yield an estimate of the characteristic residual velocity of the stars, $(K - C)\bar{r} = -5.4 \pm 0.6$ km s^{-1}, and also $K = -12.9$ km s^{-1} kpc^{-1} and $C = 16.4$ km s^{-1} kpc^{-1} (the sign has changed), which characterizes the radial component of the residual stellar velocities in the case considered. The resulting estimate, -5.4 ± 0.6 km s^{-1}, is consistent with the amplitude of the periodic radial oscillations of the stellar residual velocities in the interarm space, $f_R = 7 \pm 1$ km s^{-1}, found by Mel'nik et al. [50] based on an analysis of the motions of OB associations.

The direction of the third axis, $B_3 = 79^\circ \pm 6^\circ$, indicates compression in the Galactic plane. In fact, both roots of the deformation tensor (λ_1 and λ_2) are close to zero. This means that the compression occurs along a single axis in the direction 12°–192°, with its error being $2^\circ - 4^\circ$.

The principal axes of the residual-velocity tensor $(\sigma_1, \sigma_2, \sigma_3)$ are $(16.09 \pm 0.56, 10.04 \pm 0.53, 6.89 \pm 0.47)$ km s^{-1}, and the directions of the principal axes have the coordinates

$$l_1 = 27^\circ \pm 4^\circ, \quad b_1 = -1^\circ \pm 0^\circ,$$
$$l_2 = 117^\circ \pm 6^\circ, \quad b_2 = -1^\circ \pm 2^\circ,$$
$$l_3 = 80^\circ \pm 6^\circ, \quad b_3 = 88^\circ \pm 3^\circ.$$

We can see that the angles l_1, l_{xy}, and L_2 differ from each other, which further emphasizes the fact that the effect of the radial component is significant in the kinematics of these stars.

Figure 8c shows the distribution of the residual U, V velocities for the stars considered. The stars are

concentrated in only two peaks—the so-called Sirius and Pleiades peaks. It is striking that the velocity of the stars displaying a negative K effect relative to the local standard of rest ($v_\odot$) is fairly small.

Rybka's [51] analysis of the proper motions of about 40 000 giants of luminosity class III yielded $K = -7.5 \pm 1.8$ km s^{-1} kpc^{-1} for G5–K0 stars located beyond 250 pc (with their mean distance being about 364 pc). Our result agrees well with that of Rybka [51], leading us to conclude that the use of the high-precision space velocities of the OSACA stars has enabled us to detect this negative K effect at much closer distances. Our approach has also shown that we actually have compression along a single axis, enabling us to come closer to an understanding of the nature of this effect.

6. CONCLUSIONS

We have created and have been continuously updating the OSACA (Orion Spiral Arm Catalogue) database for stars with known coordinates, parallaxes, proper motions, and radial velocities located in the Orion arm of our Galaxy. We transformed radial velocities adopted from over 1400 sources, including the Geneva–Copenhagen survey of the solar neighborhood (CORAVEL–CfA), into a single system of radial velocities based on 854 standard stars from our list. This enabled us to calculate the weighted mean radial velocities of more than 25 000 stars of the HIPPARCOS catalog with a median error of 1 km s^{-1}. We use the elimination of systematic errors of the CORAVEL–CfA catalog as an example to demonstrate the efficiency of the proposed standard of stellar radial velocities. We have corrected numerous errors in the identification of components of multiple systems made in many publications.

We have used the OSACA data to analyze the kinematics of 6276 nearby main-sequence stars with space-velocity errors ± 2 km s^{-1}. The use of an Ogorodnikov–Milne model and analysis of the distribution of the U, V velocities the of stars revealed significant differences in the kinematics of single and multiple stars. In particular, multiple stars are much more concentrated than single stars in the vicinity of the peak associated with the Hyades–Pleiades stream in the U, V velocity plane.

Based on a sample of 9468 relatively distant ($r \approx 0.2$ kpc) stars of various spectral types, we estimated the angular velocity of the Galactic rotation to be $\omega_\circ = -25.7 \pm 1.2$ km s^{-1} kpc^{-1} (we found the vertex deviation to be $l = 13^\circ \pm 2^\circ$). The radial component of this velocity indicates a K effect, which shows up most conspicuously in the motions of A0–A5 giants. We found for the parameters of the Ogorodnikov–Milne model $K = -13.1 \pm 2.0$ km s^{-1} kpc^{-1} and $C = 14.9 \pm 2.0$ km s^{-1} kpc^{-1}, which we used to estimate the characteristic residual velocity of the stellar sample considere, -5.4 ± 0.6 km/s. The maximum compression is in the direction 12°–192° with an error of 2°–4°.

ACKNOWLEDGMENTS

We are grateful to the referee for valuable comments that contributed to the improvement of the paper. This work was supported by the Russian Foundation for Basic Research (project no. 05-02-17047).

REFERENCES

1. B. Nordström, M. Mayor, J. Andersen, et al., Astron. Astrophys. **418**, 989 (2004).
2. G. A. Gontcharov, *Order and Chaos in Stellar and Planetary Systems*, Ed. by G. G. Byrd, K. V. Kholshevnikov, A. A. Mylläri, et al., Astron. Soc. Pac. Conf. Ser. **316**, 276 ((2004)).
3. P. G. Kulikovsky, *Zvezdnaya astronomiya* (Stellar Astronomy) (Nauka, Moscow, 1985) [in Russian].
4. *The HIPPARCOS and Tycho Catalogues*, ESA SP-1200 (1997).
5. G. A. Goncharov and O. V. Kiyaeva, Pis'ma Astron. Zh. **28**, 302 (2002) [Astron. Lett. **28**, 261 (2002)].
6. F. Arenou, M. Grenon, and A. Gomez, Astron. Astrophys. **258**, 104 (1992).
7. C. Turon, M. Crézé, D. Egret, et al., *The Hipparcos Input Catalogue* (ESA Publ. Div., Noordwijk, 1992), Vols. 1–7.
8. M. Duflot, P. Figon, and N. Meysonnier, Astron. Astrophys., Suppl. Ser. **114**, 269 (1995).
9. M. Barbier-Brossat and P. Figon, Astron. Astrophys., Suppl. Ser. **142**, 217 (2000).
10. D. Bersier, G. Burki, M. Mayor, et al., Astron. Astrophys., Suppl. Ser. **108**, 25 (1994).
11. C. Fehrenbach, M. Duflot, C. Mannone, et al., Astron. Astrophys., Suppl. Ser. **124**, 255 (1997).
12. J. Fernley and T. G. Barnes, Astron. Astrophys., Suppl. Ser. **125**, 313 (1997).
13. C. Flynn and K. C. Freeman, Astron. Astrophys., Suppl. Ser. **97**, 835 (1993).
14. S. Grenier, M. O. Baylac, L. Rolland, et al., Astron. Astrophys., Suppl. Ser. **137**, 451 (1999).
15. M. Imbert, Astron. Astrophys., Suppl. Ser. **140**, 79 (1999).
16. S. Madsen, D. Dravins, and L. Lindegren, Astron. Astrophys. **381**, 446 (2002).
17. J. R. de Medeiros and M. Mayor, Astron. Astrophys., Suppl. Ser. **139**, 433 (1999).
18. J. R. de Medeiros, S. Udry, G. Burki, et al., Astron. Astrophys. **395**, 97 (2002).
19. S. M. Rucinski, C. C. Capobianco, W. Lu, et al., Astron. J. **125**, 3258 (2003).
20. E. Solano, R. Garrid, J. Fernley, et al., Astron. Astrophys., Suppl. Ser. **125**, 321 (1997).

21. J. Storm, B. W. Carney, W. P. Gieren, et al., Astron. Astrophys. **415**, 531 (2004).
22. S. Malaroda, H. Levato, and S. Galliani, Complejo Astronymico El Leoncito (2004).
23. S. Udry, M. Mayor, E. Maurice, et al., *Precise Stellar Radial Velocities*, Ed. by L. P. Ossipkov and I. I. Nikiforov, Astron. Soc. Pac. Conf. Ser. **185**, 383 (1999).
24. F. C. Fekel, *Precise Stellar Radial Velocities*, Ed. by L. P. Ossipkov and I. I. Nikiforov, Astron. Soc. Pac. Conf. Ser. **185**, 378 (1999).
25. S. Udry, M. Mayor, and D. Cueloz, *Precise Stellar Radial Velocities*, Ed. by L. P. Ossipkov and I. I. Nikiforov, Astron. Soc. Pac. Conf. Ser. **185**, 367 (1999).
26. R. P. Stefanik, D. W. Latham, and G. Torres, *Precise Stellar Radial Velocities*, Ed. by L. P. Ossipkov and I. I. Nikiforov, Astron. Soc. Pac. Conf. Ser. **185**, 354 (1999).
27. D. L. Nidever, G. W. Marcy, R. P. Butler, et al., Astrophys. J., Suppl. Ser. **141**, 503 (2002).
28. W. Dehnen and J. J. Binney, Mon. Not. R. Astron. Soc. **298**, 387 (1998).
29. S. V. M. Clube, Mon. Not. R. Astron. Soc. **159**, 289 (1972).
30. S. V. M. Clube, Mon. Not. R. Astron. Soc. **161**, 445 (1973).
31. K. F. Ogorodnikov, *Dynamics of Stellar Systems* (Fizmatgiz, Moscow, 1958; Pergamon, Oxford, 1965).
32. V. V. Bobylev, Pis'ma Astron. Zh. **30**, 861 (2004) [Astron. Lett. **30**, 785 (2004)].
33. P. P. Parenago, *Kurs zvezdnoĭ astronomii* (Course of Stellar Astronomy) (Gosizdat, Moscow, 1954) [in Russian].
34. R. J. Trumpler and H. F. Weaver, *Statistical Astronomy* (Univ. of Calif. Press, Berkeley, 1953).
35. V. V. Bobylev, Pis'ma Astron. Zh. **30**, 185 (2004) [Atron. Lett. **30**, 159 (2004)].
36. J. Skuljan, J. B. Hearnshaw, and P. L. Cottrell, Mon. Not. R. Astron. Soc. **308**, 731 (1999).
37. R. S. De Simone, X. Wu, and S. Tremaine, Mon. Not. R. Astron. Soc. **350**, 627 (2004).
38. C. A. Murray, *Vectorial Astrometry* (Hilger, Bristol, 1983).
39. V. V. Bobylev, V. V. Vityazev, and G. A. Goncharov, Vestn. Peterb. Univ., Ser. 1, issue 4, No. 25, 111 (2003).
40. R. Fux, Astron. Astrophys. **373**, 511 (2001).
41. G. Mühlbauer and W. Dehnen, Astron. Astrophys. **401**, 975 (2003).
42. C. Babusiaux and G. Gilmor, astro-ph/0501383 (2005).
43. L. R. Bedin, G. Piotto, I. R. King, et al., Astron. J. **126**, 247 (2003).
44. M. V. Zabolotskikh, A. S. Rastorguev, and A. K. Dambis, Pis'ma Astron. Zh. **28**, 516 (2002) [Astron. Lett. **28**, 454 (2002)].
45. D. Fernández, F. Figueras, and J. Torra, Astron. Astrophys. **372**, 833 (2001).
46. F. Pont, M. Mayor, and G. Burki, Astron. Astrophys. **285**, 415 (1994).
47. M. R. Metzger, J. A. R. Caldwell, and P. L. Schechter, Astron. J. **115**, 635 (1998).
48. K. Rohlfs, *Lectures in Density Waves* (Springer, Berlin, 1977; Mir, Moscow, 1980).
49. J. Torra, D. Fernández, and F. Figueras, Astron. Astrophys. **359**, 82 (2000).
50. A. M. Mel'nik, A. K. Dambis, and A. S. Rastorguev, Pis'ma Astron. Zh. **27**, 611 (2001) [Astron. Lett. **27**, 521 (2001)].
51. S. P. Rybka, Kinematika Fiz. Nebesnykh Tel **20**, 437 (2004).

Translated by A. Dambis